Eur. Phys. J. B **53**, 209–212 (2006)
DOI: 10.1140/epjb/e2006-00368-5

THE EUROPEAN PHYSICAL JOURNAL B

Electron Raman scattering in cylindrical quantum wires

X.-F. Zhao[a] and C.-H. Liu

School of Physics and Electronic Engineering, Guangzhou University, Guangzhou Higher Education Mega Center, Guangzhou 510006, P.R. China

Received 31 May 2006 / Received in final form 31 August 2006
Published online 13 October 2006 –

Abstract. Electron Raman scattering (ERS) is investigated in a free-standing semiconductor quantum wire of cylindrical geometry for two classes of materials CdS and GaAs. The differential cross section (DCS) involved in this process is calculated as a function of a scattering frequency and the radius of the cylinder. Electron states are considered to be confined within a free-standing quantum wire (FSW). Single parabolic conduction and valence bands are assumed. The selection rules are studied. Singularities in the spectra are found and interpreted for various radii of the cylinder.

PACS. 78.67.Lt Quantum wires – 78.67.-n Optical properties of low-dimensional, mesoscopic, and nanoscale materials and structures – 78.66.Fd III-V semiconductors

1 Introduction

As is known to us all, nanostructures such as supperlattices, quantum wells, quantum wires and quantum dots have been widely studied for their peculiar physical properties. Nanometer-scale confinements of the band electrons (band holes) in semiconductor materials provide varieties of quantum phenomena , such as low-dimensional electron states (hole states), modified dynamics of carriers in the systems and increased exciton binding energy [1–3]. Those quantum phenomena might be applied in the field of solid state lasers and optoelectronic devices [4].

Raman spectra is being focused on for its possible applications. Basing on resonant Raman scattering, Raman injection laser has been produced [5]. Moreover, it is well-known that Raman scattering experiments can be used to investigate different physical properties of semiconductor nanostructures [6–8]. The electronic structure of nanostructures can be investigated through Raman scattering processes considering different polarizations of incident and emitted radiation [6–9]. In connection with the experiments of the ERS, the calculation of the DCS remains a piece of fundamental work.

Multiphonon or one phonon Raman scattering has been discussed in many nanostructures [10–14]. Meanwhile, Raman scattering without phonon has also been reported, and rich spectra which are the main characteristic of the ERS have been observed [15–17]. However, the difference of the contribution of electron and hole to Raman scattering is seldom discussed. In this paper, we have calculated the DCS of Raman scattering due to electron and hole without phonon in a FSW under various radii of cylinder for the two classes of materials CdS and GaAs. The electron is completely confined within the system. Parabolic bands are also considered.

It has been found that there are anisotropic optical properties in quantum wires [18], dielectric and quantum confinement effects result in prominent exciton features such as large binding energies and oscillator strengths [19]. Similarly, in our paper, we find that dielectric and quantum confinement effects can also intensify the DCS of Raman scattering.

2 Model and theory

Let us briefly describe the model and the fundamental theory applied in our calculations. The FSW geometry is cylindrical with circular cross section of radius r_0 and length L. We consider a single conduction (valence) band split into a subband system due to electron confinement within the structure. The solution of Schrödinger equation, for an infinitely high potential barrier, is given by references [20]

$$\psi_j = \left[\sqrt{\pi L} r_0 J'_{n_j}\left(\chi_{n_j m_j}\right)\right]^{-1} J_{n_j}\left(\chi_{n_j m_j}\frac{r}{r_0}\right) \times e^{-i(n_j\phi + k_{z_j} z)} u_j \quad (1)$$

where $j = 1(2)$ stands for the electron (hole). $J_{n_j}(\chi_{n_j m_j}\frac{r}{r_0})$ is the Bessel function of order n_j, $\chi_{n_j m_j}$ denotes its zeros, $J_{n_j}(\chi_{n_j m_j}\frac{r}{r_0}) = 0$. $J'_{n_j}(\chi_{n_j m_j})$ is its partial derivative. The states are described by the quantum numbers: $n_j = 0, 1, \ldots$; $m_j = 1, 2, \ldots$. k_{z_j} is the wave number of the free motion of electron along the wire axis. u_j is the Bloch function taken at $\vec{k}_0 = 0$, where (by assumption) the band extrema are located. On the other hand,

[a] e-mail: xfzhaogz@163.com

the energy levels are determined by

$$E_j = \frac{\hbar^2}{2\mu_j}\left[k_{z_j}^2 + \left(\frac{\chi_{n_j m_j}}{r_0}\right)^2\right] \tag{2}$$

where μ_1 (μ_2) is the effective masses of electron (hole) in the wire.

3 Differential cross section

The differential cross section for electron Raman scattering of a volume V per unit solid angle $d\Omega$ for incoming light of frequency ω_l and scattering light of frequency ω_s is given by references [17]

$$\frac{d^2\sigma}{d\omega_s d\Omega} = \frac{V^2\omega_s^2\eta(\omega_s)}{8\pi^3 c^4\eta(\omega_l)}W(\omega_s,\vec{e}_s) \tag{3}$$

where $\eta(\omega)$, as a function of the radiation frequency, is the refractive index, $\vec{e}_s$ is the polarization vector for the emitted secondary radiation, c is the velocity of light in vacuum and $W(\omega_s,\vec{e}_s)$ is the transition rate calculated according to

$$W(\omega_s,\vec{e}_s) = \frac{2\pi}{\hbar}\sum_f |M_1+M_2|^2\delta(E_f-E_i) \tag{4}$$

where

$$M_j = \sum_a \frac{\langle f|\hat{H}_{js}|a\rangle\langle a|\hat{H}_{jl}|i\rangle}{E_i-E_a+i\Gamma_a} + \sum_b \frac{\langle f|\hat{H}_{jl}|b\rangle\langle b|\hat{H}_{js}|i\rangle}{E_i-E_b+i\Gamma_b}. \tag{5}$$

In equation (5), $|i\rangle$ and $|f\rangle$ denote the initial and final states of the system,respectively, their corresponding energies are E_i and E_f. $|a\rangle$ and $|b\rangle$ are the intermediate states with energies E_a and E_b while Γ_a and Γ_b are the corresponding lifetime widths. The Hamiltonian $\hat{H}_{jl}$ is

$$\hat{H}_{jl} = \frac{|e|}{\mu_0}\sqrt{\frac{2\pi\hbar}{V\omega_l}}\vec{e}_l\cdot\hat{\vec{p}} \qquad \hat{\vec{p}} = -i\hbar\vec{\nabla} \qquad j=1,2 \tag{6}$$

where μ_0 is the free-electron mass. This Hamiltonian describes the interaction between the electron and the incident radiation field in the dipole approximation. The interaction between the electron and the secondary radiation field is described by

$$\hat{H}_{js} = \frac{|e|}{\mu_j}\sqrt{\frac{2\pi\hbar}{V\omega_s}}\vec{e}_s\cdot\hat{\vec{p}} \qquad j=1,2. \tag{7}$$

This Hamiltonian describes the photon emitted by the electron (hole) when transitions between conduction (valence) subbands of the system occur.

There are two possible processes of ERS [17]:

(1) The intermediate states are in the conduction band. An electron-hole pair (EHP) between the state $|n_2,m_2\rangle$ in the valence band and the state $|n_1^{'},m_1^{'}\rangle$ in the conduction band is created when absorbing an incident light quantum. Then an electronic transition from the state $|n_1^{'},m_1^{'}\rangle$ to the state $|n_1,m_1\rangle$ in the conduction band occurs to emit a scattered photon.

(2) The intermediate states are in the valence band. The ERS process involves two electrons: one electron moves from the state $|n_2^{'},m_2^{'}\rangle$ in the valence band to the state $|n_1,m_1\rangle$ when absorbing an incident photon, the other electron transfers from the state $|n_2,m_2\rangle$ to the vacant state in the $|n_2^{'},m_2^{'}\rangle$ subband. In fact, the final effect is that an electron shifts from the state $|n_2,m_2\rangle$ to the state $|n_1,m_1\rangle$.

In the initial state $|i\rangle$, it has a completely occupied valence band, an unoccupied conduction band, and an incident photon of energy $\hbar\omega_l$. Thus,

$$E_i = \hbar\omega_l. \tag{8}$$

The final state $|f\rangle$ contains an EHP excited in a real state and a secondary radiation emitted photon of energy $\hbar\omega_s$. Hence,

$$E_f = E_{n_1m_1} + E_{z_1} + E_{n_2m_2} + E_{z_2} + \hbar\omega_s + E_g. \tag{9}$$

For the intermediate states $|a\rangle$ and $|b\rangle$, the energies E_a and E_b can be easily obtained from the above discussion, and using energy and momentum conservation laws, we can evaluate the denominators in equation (5)

$$E_i - E_a = E_{n_1m_1} - E_{n_1^{'}m_1^{'}} + \hbar\omega_s \tag{10}$$

$$E_i - E_b = E_{n_2^{'}m_2^{'}} - E_{n_2m_2} - \hbar\omega_s. \tag{11}$$

Now, we can calculate the matrix elements. Considering the allowed electron transitions between conduction and valence bands, equations (1) and (6), the matrix element $\langle a|\hat{H}_{jl}|i\rangle$, in the envelope function approximation, can be written as

$$\langle a|\hat{H}_{jl}|i\rangle = \frac{i\mu_1|e|}{\mu_0}\sqrt{\frac{8\pi}{\hbar V\omega_l}}\frac{W_{n_1^{'}n_2}}{r_0^2 J'_{n_1^{'}}(\chi_{n_1^{'}m_1^{'}})J'_{n_2}(\chi_{n_2m_2})} \times\int J_{n_1^{'}}\left(\chi_{n_1^{'}m_1^{'}}\frac{r}{r_0}\right)\vec{e}_l\cdot\vec{r}J_{n_2}\left(\chi_{n_2m_2}\frac{r}{r_0}\right) \times rdr\delta_{n_1^{'},n_2}\delta_{k_{z_i},k_{z_a}}. \tag{12}$$

For the electron(hole)-secondary-radiation interaction matrix element, it can be seen that

$$\langle f|\hat{H}_{js}|a\rangle = i|e|\sqrt{\frac{8\pi}{\hbar V\omega_s}}\frac{W_{n_1n_1^{'}}}{r_0^2 J'_{n_1}(\chi_{n_1m_1})J'_{n_1^{'}}(\chi_{n_1^{'}m_1^{'}})} \times\int J_{n_1}\left(\chi_{n_1m_1}\frac{r}{r_0}\right)\vec{e}_s\cdot\vec{r}J_{n_1^{'}}(\chi_{n_1^{'}m_1^{'}}\frac{r}{r_0}) \times rdr\delta_{n_1,n_1^{'}}\delta_{k_{z_f},k_{z_a}}. \tag{13}$$

Thus, for the intermediate states in the conduction band, we get the DCS for ERS, that is

$$\frac{d^2\sigma}{d\omega_s d\Omega} = \frac{16\omega_s\eta(\omega_s)e^4\mu_1^2}{\omega_l\eta(\omega_l)c^4\hbar^3 r_0^8\mu_0^2}\frac{1}{(E_i-E_a)^2+\Gamma_a^2}|Y_1|^2|Y_2|^2 \tag{14}$$

where

$$Y_1 = \frac{W_{n_1' n_2}}{J'_{n_1'}\left(\chi_{n_1' m_1'}\right) J'_{n_2}(\chi_{n_2 m_2})} \times \int J_{n_1'}\left(\chi_{n_1' m_1'}\frac{r}{r_0}\right)\vec{e}_l \cdot \vec{r} J_{n_2}\left(\chi_{n_2 m_2}\frac{r}{r_0}\right) r dr$$

$$Y_2 = \frac{W_{n_1 n_1'}}{J'_{n_1}(\chi_{n_1 m_1}) J'_{n_1'}(\chi_{n_1' m_1'})} \times \int J_{n_1}\left(\chi_{n_1 m_1}\frac{r}{r_0}\right)\vec{e}_s \cdot \vec{r} J_{n_1'}\left(\chi_{n_1' m_1'}\frac{r}{r_0}\right) r dr$$

$$W_{n_1' n_2} = \frac{\hbar^2}{2\mu_1}\left(\frac{\chi_{n_1' m_1'}}{r_0}\right)^2 - \frac{\hbar^2}{2\mu_2}\left(\frac{\chi_{n_2 m_2}}{r_0}\right)^2$$

$$W_{n_1 n_1'} = \frac{\hbar^2}{2\mu_1}\left[\left(\frac{\chi_{n_1 m_1}}{r_0}\right)^2 - \left(\frac{\chi_{n_1' m_1'}}{r_0}\right)^2\right].$$

We can get similar expressions for the interband ERS process with the intermediate states in the valence band (with replacements $n_2 \to n_1$, $n_1' \to n_2'$, $n_1 \to n_2$; $m_2 \to m_1$, $m_1' \to m_2'$, $m_1 \to m_2$; $\mu_1 \to \mu_2$, $\mu_2 \to \mu_1$).

4 Results and discussions

In this section, the differential cross section (DCS) given by equation (14) is calculated numerically for a FSW of GaAs or CdS. The physical parameters used in our expressions are [13,14,20]: $\Gamma_a = \Gamma_b = 1$ meV; $\mu_1 = 0.067\mu_0$, $\mu_2 = 0.45\mu_0$, $\varepsilon = 13.18$ and $E_g = 1.5177$ eV for GaAs ; while $\mu_1 = 0.18\mu_0$, $\mu_2 = 0.51\mu_0$, $\varepsilon = 8.9$ and $E_g = 2.6$ eV for CdS. In our calculations, we select quantum numbers: $n_1 = n_1' = n_2' = n_2 = 0$.

In the case of the scattering configuration $\bar{Z}(\vec{e}_l, \vec{e}_{sz})X$, the following selection rule is satisfied: $n_1 = n_2$. In this case, it can be seen from equations (10) or (11), the emission spectra of the ERS show maxima for the value of ω_s given by

$$\omega_s = \frac{E_{n_1' m_1'} - E_{n_1 m_1}}{\hbar} \tag{15}$$

or

$$\omega_s = \frac{E_{n_2' m_2'} - E_{n_2 m_2}}{\hbar}. \tag{16}$$

So we can obtain the information about electronic (hole) states involved in the scattering process. Electron transitions are indicated by $\nu_e(m_2, m_1', m_1)$ and $\nu_h(m_1, m_2', m_2)$ corresponding to conduction electron and valence hole intersubband transitions.

In Figure 1a, we show the emission spectra of the FSW due to hole in the scattering configuration $\bar{Z}(\vec{e}_l, \vec{e}_{sz})X$. We select the radius $r_0 = 4$ nm. It can be observed: the positions of singularities for the two classes of materials CdS and GaAs are different; in the same condition, the value of singularity for a GaAs system is smaller than that for a CdS system.

Similar to Figure 1a, in Figure 1b, we show the emission spectra of the FSW due to electron with $r_0 = 4$ nm.

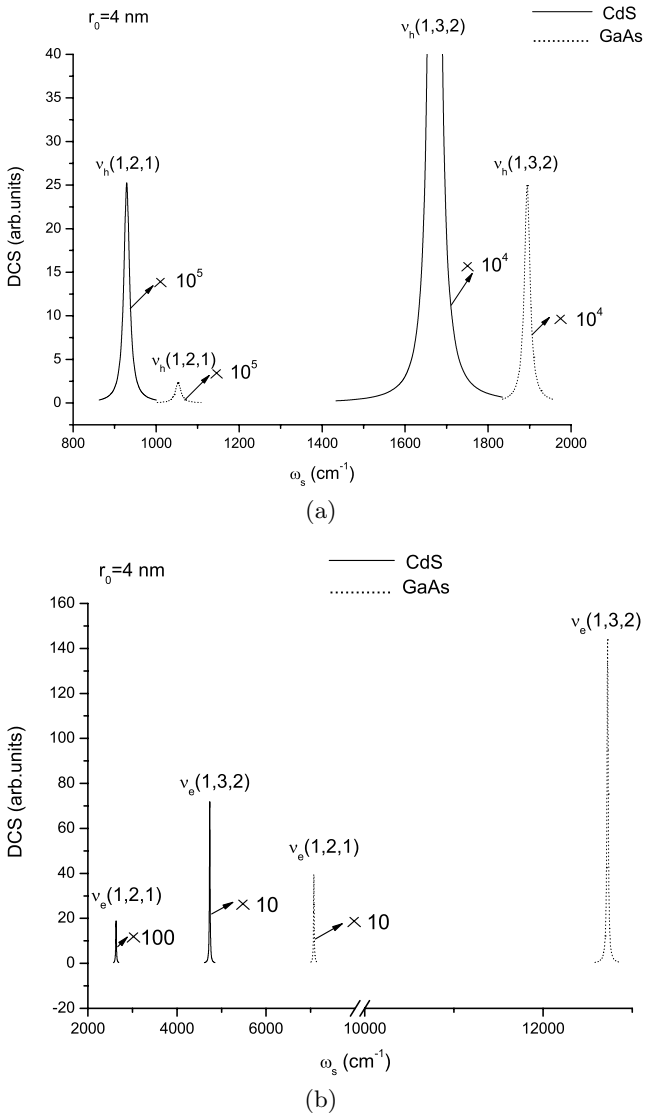

Fig. 1. Raman spectra of the FSW due to hole/electron in the scattering configuration $\bar{Z}(\vec{e}_l, \vec{e}_{sz})X$ for a CdS/GaAs system with $r_0 = 4$ nm. (a) hole (b) electron.

It can be obtained: in the same condition, the value of singularity for a GaAs system is larger than that for a CdS system. This is caused by dielectric confinement. A larger dielectric constant for a GaAs system leads to its a larger value of singularity, which is similar to the Figure 2 in references [21]. Compare Figure 1a to Figure 1b we can easily find: the value of singularity due to hole(electron) is different for different materials, in the same condition, the value of singularity due to hole(electron) for a GaAs system is smaller(larger) than that for a CdS system; in the same system, the value of singularity due to electron is larger than that due to hole and this is accord with the Figure 2 in references [17].

In Figures 2a and 2b, for a GaAs system, we show the emission spectra of the FSW due to hole and electron, respectively. There appears rich spectra like that mentioned in references [17]. We can see that the value of singularity due to both hole and electron becomes larger when the

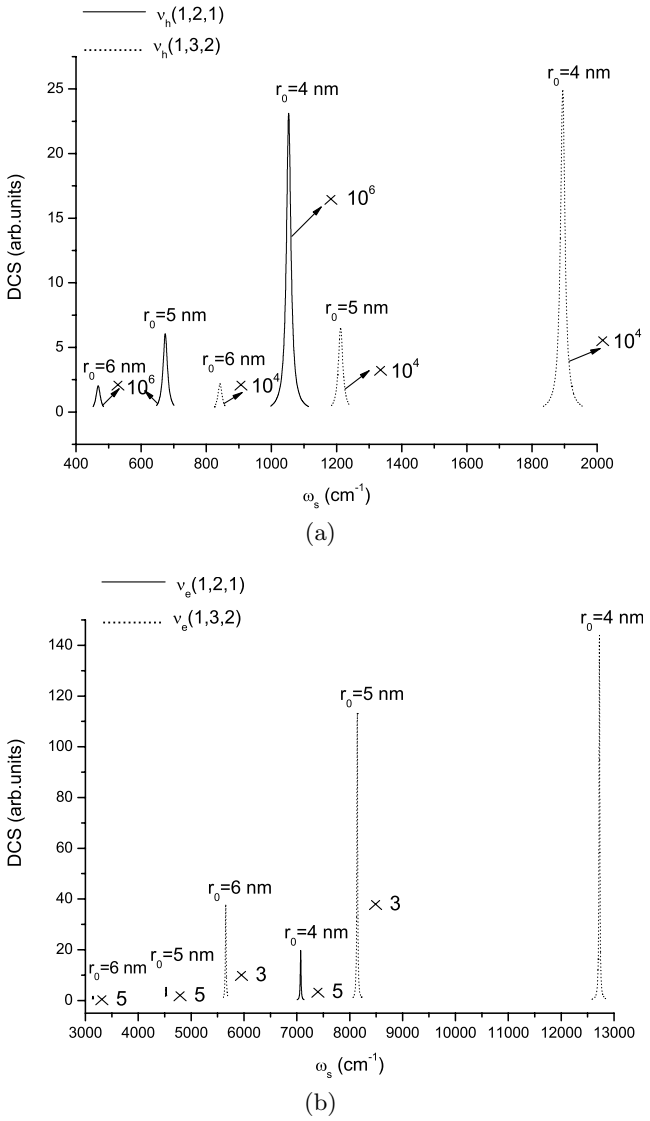

Fig. 2. Raman spectra of the FSW due to hole/electron in the scattering configuration $\bar{Z}(\vec{e}_l, \vec{e}_{sz})X$ for a GaAs system with various radii. (a) hole (b) electron.

radius of cylinder becomes smaller. This is caused by a very anisotropic optical activity due to quantum confinement [22,23]: the DCS parallel to the wire axis is dominant due to the anisotropic optical activity, the smaller the radius becomes, the stronger the anisotropic optical activity becomes due to the more significant quantum confinement, so the value of singularity related to both hole and electron increases which likes Figure 6b in reference [19]. However, as discussed above, with the same radius, the contribution to Raman scattering due to electron is far larger than that due to hole.

5 Conclusions

We have investigated theoretically the DCS for the ERS process associated with electron and hole in a free-standing semiconductor quantum wire of cylindrical geometry for the two classes of materials CdS and GaAs. The numerical results in the scattering configuration $\bar{Z}(\vec{e}_l, \vec{e}_{sz})X$ show that the DCS depends on the radius r_0 and it varies in different systems. In the same condition, the value of singularity due to electron(hole) for a GaAs system is larger(smaller) than that for a CdS system for the sake of dielectric confinement. The contribution to Raman scattering due to electron or hole increases as the radius of the cylinder decreases which is caused by quantum confinement of the FSW. However, with the same radius, the contribution due to electron is far larger than that due to hole.

This work is supported by Guang-dong Provincial Natural Science Foundation of China(under Grant No. 05001873).

References

1. E.R. Margine, V.H. Crespi, Phys. Rev. Lett. **96**, 196803 (2006)
2. S.H. Anastasiadis, K. Karatasos, G. Vlachos, Phys. Rev. Lett. **84**, 915 (2000)
3. T. Otterburg, D.Y. Oberli, M.-A. Dupertuis, N. Moret, E. Pelucchi, B. Dwir, K. Leifer, E. Kapon, Phys. Rev. B. **71**, 033301 (2005)
4. C.Z. Ning, Phys. Rev. Lett. **93**, 187403 (2004)
5. M. Troccoli, A. Belyanin, F. Capasso, E. Cubukcu, D.L. Sivco, A.Y. Cho, Nature **433**, 845 (2005)
6. M. Cardona, G. Güntherodt, *Light Scattering in Solid V*, Spinger Topics in Applied Physics, Vol. 66 (Heidelberg, Springer, 1989)
7. M. Cardona, Superlatt. Microstruct. **7**, 183 (1990)
8. M.V. Clein, IEEE J. Quantum Electron. **22**, 1760 (1986)
9. A. Pinczuk, E. Burstein, *Light Scattering in Solid I*, Spinger Topics in Applied Physics, Vol. 8 (Heidelberg, Springer, 1983)
10. T. Ruf, M. Cardona, Phys. Rev. Lett. **63**, 2288 (1989)
11. R. Rodríguez-Suárez, E. Menéndez-Proupin, Phys. Rev. B. **62**, 11006 (2000)
12. A.G. Milekhin, A.I. Toropov, A.K. Bakarov, D.A.Tenne, Phys. Rev. B **70**, 085314 (2004)
13. R. Betancourt-Riera, R. Betancourt, R. Rosas, R. Riera, J.L. Marín, Physica E **24**, 257 (2004)
14. C.H. Liu, B.K. Ma, C.Y. Chen, Chin. Phys. **11**, 0730 (2002)
15. F. Geerinckx, F.M. Peeters, J.T. Devreese, J. Appl. Phys. **68**, 3435 (1990)
16. P. Maksym, T. Chakraborty, Phys. Rev. Lett. **65**, 108 (1990)
17. T.G. Ismailov, B.H. Mehdiyev, Physica E **31**, 72 (2006)
18. M. Ogawa, M. Ito, S. Fukushima, T. Miyoshi, Solid-State Electronics **42**, 1205 (1998)
19. K. Chernoutsan, V. Dneprovskii, S. Gavrilov, V. Gusev, E. Muljarov, S. Romanov, A. Syrnicov, O. Shaligina, E. Zhukov, Physica E **15**, 111 (2002)
20. J.M. Bergues, R. Betancourt-Riera, R. Riera, J.L. Marín, J. Phys.: Condens. Matter **12**, 7983 (2000)
21. G. Goldoni, F. Rossi, A. Orlandi, M. Rontani, F. Manghi, E. Molinari, Physica E **6**, 482 (2000)
22. L. Dorigoni, O. Bisi, F. Bernardini, S. Ossicini, Phys. Rev. B. **53**, 4557 (1996)
23. S. Ossicini, L. Dorigoni, O. Bisi, Appl. Surface Sci. **102**, 395 (1996)